A simple realistic driver model

A Simple Realistic Driver Model

Matthew C Best
Dept of Aeronautical and Automotive Engineering
Loughborough University

Ashby Road, Loughborough, Leicestershire, LE11 3TU, UK
Tel: (+44) 1509 227209 Fax: (+44) 1509 227275
E-mail : m.c.best@lboro.ac.uk

Many of the published driver models concentrate on algorithms which achieve accurate path following at the expense of realistic replication of the driving task itself. In this paper we consider only the most basic driving responses, to achieve a simple yet surprisingly realistic driver model. Lateral control is based on steering corrections aimed at projecting the vehicle onto a path at a single preview point on the road ahead. Only the preview time and a single proportional gain are required parameters, supported by a basic approximation of understeer gradient which becomes proressively more important as desired lateral acceleration increases. The longitudinal model regulates speed solely in proportion to an estimate of the length of road the driver can see ahead. Both aspects of the model are executed in a computationally efficient way, using the simplest possible definition of a track. The model is tested for robustness in simulation, and it gives intuitively sensible responses. Results are then given in comparison to vehicle tests, with the longitudinal parameters tuned to match the measured driving behaviour of two test subjects, while nominal lateral parameters are shown to be effective. Finally, the model is also shown to be capable of reasonable, if approximate prediction of speed variations for the same test drivers on an independent section of road.

Topics / Driver Model

1. INTRODUCTION

Driver models are widely used for simulation, optimisation, proving chassis control algorithms and in the development of Advanced Driver Assistance Systems (ADAS) and autonomous vehicles. For many of these applications the model is primarily required for path following, so the objective is often geared to this end; as a result successful tracking algorithms can be confused with models of driver behaviour. Here we consider a model of driver behaviour, both longitudinal and lateral, in the absence of traffic, on open, winding country roads.

Driving is an easy task – particularly in the control of steering at normal driving speeds. Even novice drivers can get into a car they have never driven before (with an unknown steering ratio) and drive it immediately, without significant path error. Consequently, many of the driver models proposed to date seem disproportionately complicated; the most popular, by Macadam [1] and later Sharp et al [2] consider multiple reference points, with the latter coupling these with yaw rate feedback in an optimal controller. Ungoren and Peng [3] consider a similar approach, and they also note the complexity and diversity of recently published work in a useful literature review. Others require knowledge of the vehicle dynamic model (eg [4]), and the author has previously considered a complex vector field approach to path planning, in [5].

While these models achieve accurate path tracking, and may be able to replicate expert driving and driving near the handling limit, their algorithms aren't representative of normal, unskilled drivers, for whom the vast majority of ADAS systems (for example) are developed. Other simplified driver models have been presented – eg [6], but these are used most widely in the context of vehicle aerodynamics, where the test environment invariably considers exclusively straight line paths.

This paper considers the fundamental control task of driving, at a basic level, and models the key features in a very simple form. The two associated benefits of the approach are that it is easy to implement, and more representative of average driving.

The lateral and longitudinal control models are described with reference to physical behaviours of drivers, in Section 3. A vehicle model (briefly described in Section 2) is then used to explore the viable range of operation of the driver model, in Section 4. Finally vehicle test results are given to demonstrate validity and acccuracy, and show how the new model's parameters can be tuned to real driving behaviour, in Section 5.

2. VEHICLE MODEL

The vehicle is modelled as a rigid body, free to move in six degrees of freedom under the influence of tyre and nominal drag forces on a flat road.

Tyre forces are found from a combined slip Pacejka formula based on lateral and longitudinal slips computed from the velocity vectors at the contact patches. These forces vary appropriately with vertical

load, which is computed assuming a linear spring-damper suspension compensated by suspension link forces that act at static roll centres. Four wheel spin degrees of freedom are modelled, driven by input drive torque τ shared equally at the front wheels. This is reacted by the longitudinal tyre forces and a nominal road drag. A full description of the tyre model is available in [5]. The vehicle parameters are nominal but consistent with a medium sized passenger vehicle, sourced from [7].

Vehicle position and orientation in global coordinates are calculated using yaw rate r, and forward and lateral speeds u, v :

$$\dot{\gamma} = r$$
$$\begin{pmatrix} \dot{X} \\ \dot{Y} \end{pmatrix}_G = \begin{bmatrix} \cos\gamma & -\sin\gamma \\ \sin\gamma & \cos\gamma \end{bmatrix} \begin{pmatrix} u \\ v \end{pmatrix} \quad (1)$$

3. DRIVER MODEL

3.1 Lateral Behaviour

When driving, I am conscious of tracking one point on the road ahead and continuously adapting the steering to keep the vehicle on a path toward that point. The amount of preview varies with speed, so a finite preview time, T_p seems appropriate. For straight line driving this requires a simple lateral deviation correction process, and interestingly the same is also true on a fixed radius curve; small corrections are needed to the steady-state steer. The basis of lateral control here is therefore forward prediction of vehicle position based on current steer angle; the driver is only expected to have developed an appreciation of what radius a given steer angle will deliver, in the steady-state, over T_p.

A particular problem with driver modelling is accurate but computationally simple respresentation of the road. Smooth, eg. circular or splined road segments provide a continuous reference, but are computationally burdensome. Here we will principally rely on the simplest road reference, a linearly interpolated trace of X,Y locations for a prescribed simulated track, or from GPS measurements. However this driver model method also lends itself well to circular road segments, so both alternatives are documented. Fig 1 illustrates the evaluation of signed lateral error at the preview point P.

The control operates discretely; from the known global position of the vehicle CG, G, orientation ψ, speed u and steered wheel angle δ at time step k. The forward path radius under fixed steer angle and constant speed is, from the well known steady-state handling equation,

$$R = \frac{L + K_{ug} u^2(k)/g}{\delta(k)} \quad (2)$$

Unit vectors are, by rotation of the global X facing vector through ψ

$$\hat{t}_G = \begin{pmatrix} \cos\psi \\ \sin\psi \end{pmatrix}, \quad \hat{n}_G = \begin{pmatrix} -\sin\psi \\ \cos\psi \end{pmatrix} \quad (3)$$

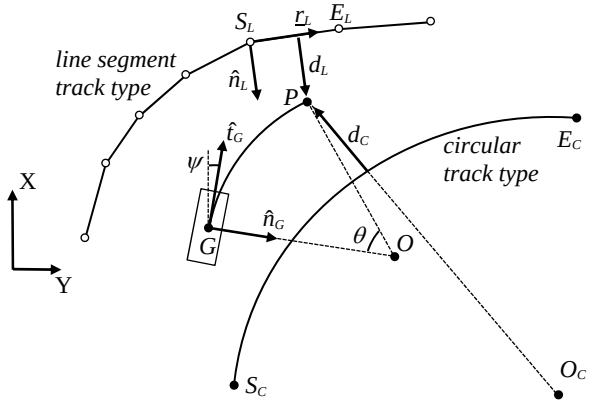

Fig. 1 : Calculation of preview point and lateral deviation from both linear and circular track types

and angle traversed along the arc is

$$\theta = u(k) T_p / R \quad (4)$$

One way to locate point P is via the arc centre O,

$$P = G + R\hat{n}_G - \begin{pmatrix} \cos\theta & -\sin\theta \\ \sin\theta & \cos\theta \end{pmatrix} R\hat{n}_G \quad (5)$$

The signed deviation from a circular track segment, d_c is then simply

$$d_C = R_C - |P - O_C| \quad (6)$$

and the validity of the particular segment can be confirmed by P satisfying

$$\begin{aligned} &(S_C - O_C) \times (P - O_C)\big|_z > 0 \quad \text{AND} \\ &(E_C - O_C) \times (P - O_C)\big|_z < 0 \end{aligned} \quad (7)$$

with notation $|_z$ signifying the z component of the appropriately (3d expanded) vector products.

For the linear segment track type,

$$d_L = (P - S_L).\hat{n}_L \quad (8)$$

where, for a valid segment

$$0 < |(P - S_L).\hat{r}_L| < |r_L| \quad (9)$$

Here the smallest valid d_L will be approprate, but two snags arise in that (a) checking all segments is computationally expensive, and (b) since the line segment track is discontinuous in gradient, conditions can arise where two, or zero valid segments can exist. To avoid both problems, take advantage of the fact that P will only progress forward along the track, so retaining i as the number of the previously valid track segment, at each new control step

$$\text{while} \quad |(P - S_L(i)).\hat{r}_L(i)| > |r_L(i)|, \; i = i+1 \quad (10)$$

Steering control is based solely on correction of the current value, given the predicted future point error d (evaluated as d_c or d_L above as appropriate),

$$\delta(k+1) = \delta(k) + K_{lat} d \tag{11}$$

3.2 Longitudinal Behaviour

From trial data for unimpeded natural driving on minor roads, it is clear that speed varies with lookahead distance – the amount of road ahead that is visible. Monitoring this (apparently quite sensitive) variable accurately requires knowledge of the track ahead and the orientation and visual range of the driver. A suitable compromise between accuracy and simplicity is achieved using the criteria illustrated in Fig 2.

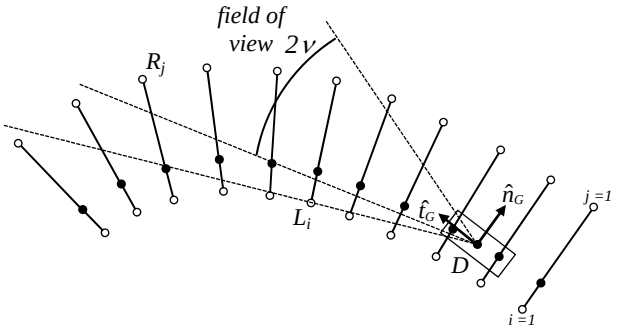

Fig. 2 : Logic used to define forward view

Left and right road boundary markers are pre-defined at each track point as illustrated, using path normals, road width and respecting the side of the road traversed (left, illustrated, in the UK). Point *D* can reasonably be approximated at the vehicle CG, but is more accurately,

$$D = G + \varepsilon \hat{n}_G \tag{12}$$

where ε represents the left or right offset of the driver's seated position.

Denoting left index *i* and right index *j*, the most extreme visible points L_i and R_j are identified, and for computational efficiency a similar process to eqn (10) is adopted; it is assumed *i* and *j* can only increase.

Ignoring field of view initially, points *L* and *R* can each increase independently of one another, provided vectors DL_i and DR_j do not pass an apex (conditions C_1, C_2) or cross each other (condition C_3) :

$$C_1 = (L_i - G) \times (L_{i+1} - G)\big|_z > 0$$
$$C_2 = (R_j - G) \times (R_{j+1} - G)\big|_z < 0$$
$$C_3 = (L_{i+1} - G) \times (R_{j+1} - G)\big|_z > 0$$

while (C_1 OR C_2) AND C_3, if C_1, $i = i+1$ (13)

while (C_1 OR C_2) AND C_3, if C_2, $j = j+1$ (14)

This logic will always increase one side to the next corner apex (L_i illustrated) and the other side to the furthest point that does not cross the same line (DL_i extended, illustrated). Note that in Fig. 2, by this criteria alone, R_j would be one point further along. For long lookahead distances this is sufficient, but within corners it can result in a large angle between the assumed line of sight and the vehicle orientation, just at the point when the driver is concentrating on the corner. To restrict according to a constrained field of view, 2ν, define

$$\underline{r}_{RV} = \hat{t}_G + \tan(\nu)\hat{n}_G, \quad \underline{r}_{LV} = \hat{t}_G - \tan(\nu)\hat{n}_G \tag{15}$$

and note that since we are only interested in point *R* or *L* which is furthest away, we only need to consider *R* increasing beyond the left field of view (illustrated), or *L* beyond the right. In eqn (13) add the caveat that

if $(L_i - G) \times \underline{r}_{RV}\big|_z > 0$ AND $(L_{i+1} - G) \times \underline{r}_{RV}\big|_z \le 0$

then no further increase of *i* is permitted within the current iteration of the controller, and for eqn (14),

if $(R_j - G) \times \underline{r}_{LV}\big|_z < 0$ AND $(R_{j+1} - G) \times \underline{r}_{LV}\big|_z \ge 0$

j is similarly restricted. The single lookahead distance that should be used in conjunction with this logic is,

if *j* is restricted, $d_{long} = |R_j - G|$

if *i* is restricted, $d_{long} = |L_i - G|$ (16)

otherwise, $d_{long} = \max(|R_j - G|, |L_i - G|)$

This is converted to a demand speed by a simple linear relationship,

$$u_{dem} = K_{long} d_{long} + u_0 \tag{17}$$

and u_{dem} is saturated at u_{max}, to accommodate long lookahead distances sensibly.

A proportional controller is sufficent to model the delay between driver demand and the speed of the vehicle, though two gains are used, so slowing down is modeled independently of speeding up, since the former naturally tends to be more urgent. For the vehicle model used here, these gains are scaled to determine total torque shared between the driven wheels,

$$\tau = K_{p-}(u_{dem} - u), \quad u_{dem} < u$$
$$\tau = K_{p+}(u_{dem} - u), \quad u_{dem} > u \tag{18}$$

In summary, the lateral controller is defined by just two parameters, preview time T_p and steering gain K_{lat}, and the longitudinal control depends on field of view ν (which is relatively insensitive, and set to a nominal 10° here), speed demand scaling K_{long}, u_0, saturation u_{max} and the proportional gains K_{p+} and K_{p-}.

4. ROBUSTNESS STUDY IN SIMULATION

The lateral control is examined in simulation at constant forward speeds by execution of an ISO single lane-change manoeuvre (3.5m lateral shift over 30m length). A nominal smooth path is set using straight line start and end segments linked by two 13.3° circular arcs with radius 65m. This is then approximated by straight line segments at a track spacing of 0.6m or 6m. Fig. 3 illustrates the effect of track spacing, along with various choices of T_p, K_{lat} and K_{ug} for the vehicle model as it maintains a cruise speed of 50kph (13.9m/s). The

control sampling rate is 100Hz for all results in this paper, to emulate the continuous nature of normal driving control. For easier comparison, all data in the results Sections are plotted relative to distance along the track.

road disc^n *(m)*	T_p *(s)*	K_{lat}	K_{ug} *(°/g)*	legend
0.6	0.5	0.2	0	baseline
6	0.5	0.2	0	coarse road
0.6	0.5	0.02	0	low gain
0.6	0.5	0.2	1	known usg
0.6	0.25	0.8	0	tight control

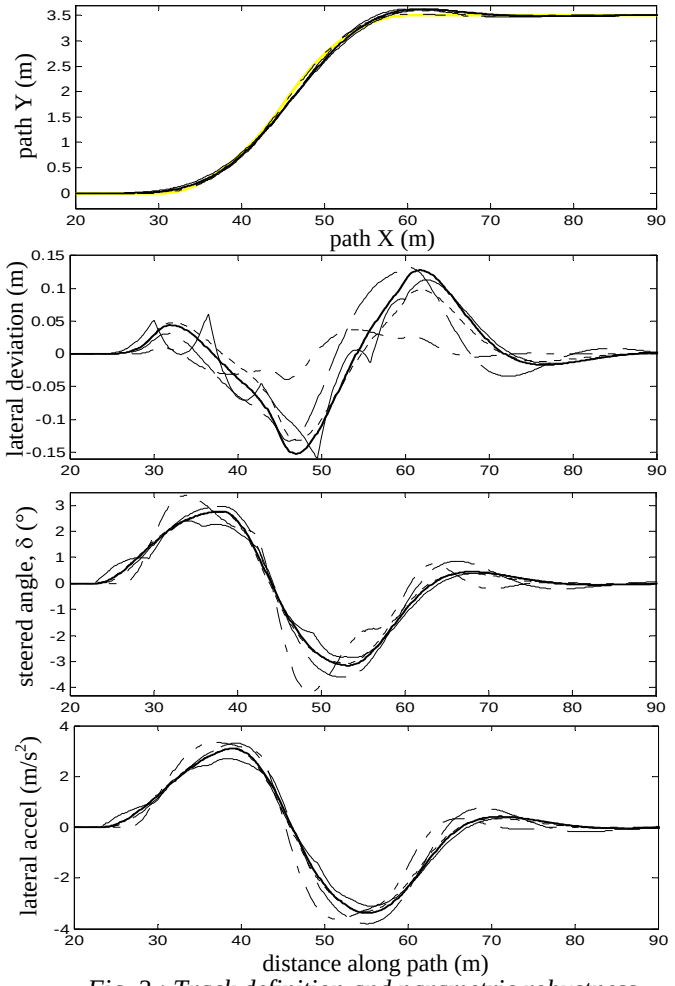

Fig. 3 : Track definition and parametric robustness

All cases show good path following, with lateral errors peaking at around 15cm. All the results use the simpler line segment track definition and smooth steer behaviour results, provided a reasonably fine spacing is used; the 6m case shows how steering becomes jerky when wider spacing is used. The very discontinuous lateral errors for this case are due to track approximation rather than CG path error. The algorithm remains stable for values of K_{lat} anywhere in the illustrated region 0.02 – 0.2; K_{lat} significantly below 0.02 causes instability in steer angle, and above 0.2 we see high frequency ringing in steer.

The illustrated lower gain case exhibits expected lower steer magnitude initially, followed by slightly higher steer as the error at lookahead point *P* is allowed to become larger. Note that CG error, although phased differently to the baseline case, does not change significantly in magnitude. K_{lat} is thus not a sensitive parameter, and this reflects real driving; there is only one sensible steer solution for any given path.

Lookahead times are successful anywhere between 0.2 – 0.7s (not illustrated); at this speed this range is 1 – 4 car lengths, which surely includes all reasonable values. High T_p causes corner-cutting, and low T_p, although arguably less realistic, can be coupled with higher K_{lat} to achieve very low lateral error; an extreme case is illustrated. Fig. 3 shows 'driver knowledge' of the understeer gradient has little effect on control outcome at this speed – a slightly lower lateral error results. The model here is very close to neutral in the linear region of the tyres, with K_{ug} ~ 1°/g.

speed, *u*	K_{ug} *(°/g)*	legend
20	0	baseline
20	5	approximated
25	5	understeer
30	5	

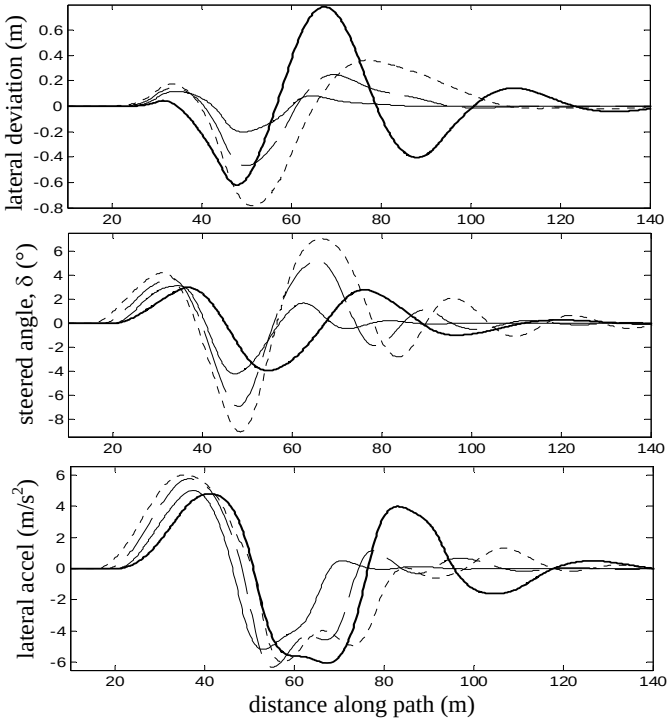

Fig. 4 : Speed and understeer gradient robustness

Fig. 4 shows cases where the constant speed is increased. For all these results K_{lat} = 0.1 and T_p = 0.5. With K_{ug} = 0 in the driver model, 20m/s is the fastest achieveable speed. But with K_{ug} nominally estimated for the nonlinear range, at 5°/g, the model is successful at much higher speeds – even beyond 50m/s in this simulation study.

As speed increases, the steer inputs become excessive and the corners are progressively cut to give high lateral errors, but the control remains stable. This suggests that an understeering car can be driven to higher lateral acceleration using the given simple driver model, provided a basic allowance is made for steering

sensitivity. Again this is consistent with real driving behaviour.

5. VEHICLE RESULTS

The driver model is validated against test drives conducted on clear sections of single carriageway country road chosen for their combination of straights and corners of varying curvature. The total road width varied between 5.5 and 7m, with the majority close to 6m, so left and right boundary markers were fixed at -1.5m, +4.5m respectively. Position and speed of the Jaguar XF test vehicle were acquired from a high quality INS and GPS system, and steered wheel angle was taken from the standard vehicle CAN signal for steering wheel, converted using the known steering rack gain map. The vehicle is left-hand drive, so ε is set at -0.38.

Sections of test track were established by taking median GPS data from three test runs driven at 10m/s. Data from the selected run was then sampled with approximately 2m spacing to define the path in short line segments. Fig 5(a) illustrates both directions of travel for one of the resulting test sections, confirming good accuracy; the small degree of low frequency drift error does not influence the validation.

Five drivers were asked to drive normally, however they felt most comfortable, over four sections of road in each direction. Fig. 5 summarises results and tuning of the longitudinal model, on one of these sections.

In Fig 5 (b) drivers 'M' and 'G' show the two extremes of speed control behaviour that were observed. G drives faster on straight sections and brakes to lower speeds on corners, whereas M maintains lower speed variance. The solid lines here show how the longitudinal model was tuned to match the test data as closely as possible. Given that the parameters influence change in speed relatively independently, this is easily done by eye; phase errors make formal optimisation more difficult. The resulting full parameter set for each driver is given in Table 1; note that the lateral parameters are nominal; no tuning is necessary.

Given the multitude of visual and other cues which will influence a given driver's speed, the simple longitudinal model should not be expected to map speed exactly. Why, for example does M drive more slowly on the long straight, but faster on a later, shorter one? The longitudinal model is able to match the essential speed control behaviour reasonably well, and the difference in driving style is captured.

Lateral deviation and steer are shown for driver G in Figs 5(c),(d). The behaviour for all drivers is almost identical, which is consistent with the comments made in Section 4, so it is not necessary to show both driver's steer results. Note that the vehicle model is not tuned to match the test vehicle, though clearly its understeer gradient is similar; the steer traces are almost identical.

	T_p	K_{lat}	K_{ug}	K_{long}	u_0	u_{max}	K_{p+}	K_{p-}
M	0.5	0.1	1	0.10	10	22	70	500
G	0.5	0.1	1	0.17	4.5	26	100	500

Table 1 : Tuned model parameters for drivers M and G

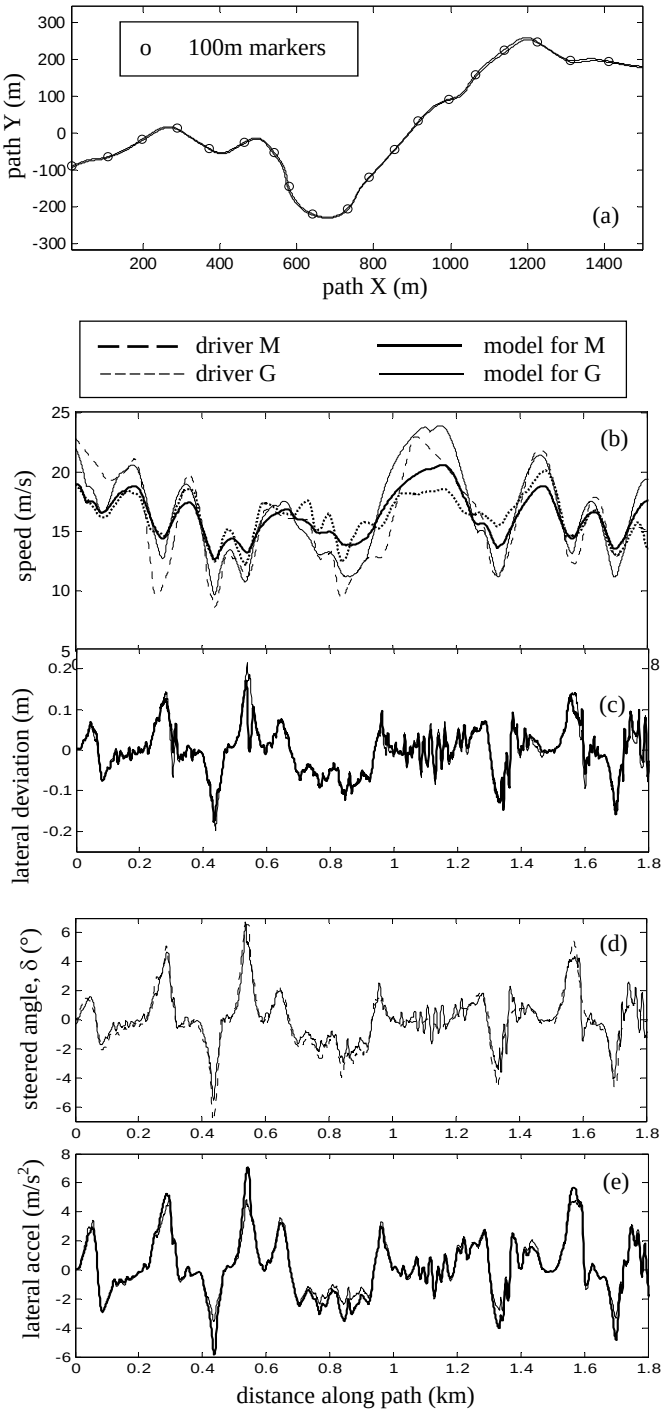

Fig. 5 : Driver model vs vehicle test data (design)

Peak lateral deviation is just over 0.2m, always in the sense of cutting the corner slightly; this is realistic. The overall width of the test vehicle (excluding wing mirrors) is 1.94m, so total deviation would need to exceed 0.5m for part of the vehicle to cross the centre

line of a 6m road. Note of course that when driving, the path the driver 'sights' is not necessarily the centre of the lane, particularly on corners, so this will account for some further deviation in practice.

Lateral accelerations in Fig 5(e) peak at around $7m/s^2$ for M and $5m/s^2$ for G; although slower on average, M carries more speed into the corners. The model caters well despite operating in the nonlinear region of the tyres.

Some sharply oscillatory steering, particularly between 1000m and 1200m is interesting; this is caused by lack of smoothness in the test track data, and is a similar phenomenon to the 6m spaced track results of Section 4 (note how lateral errors oscillate, though vehicle path does not deviate significantly through this straight section).

Finally, Fig. 6 shows speed results, measured and driver modeled, for drivers M and G on a different section of road, with the model retaining the parameters of Table 3. Higher speeds can be achieved on this road, and the simplistic nature of speed demand saturation in the driver model is apparent here. The essential difference in speed control style is still seen however, and the lateral control is equally effective on this, and indeed all the road sections tested.

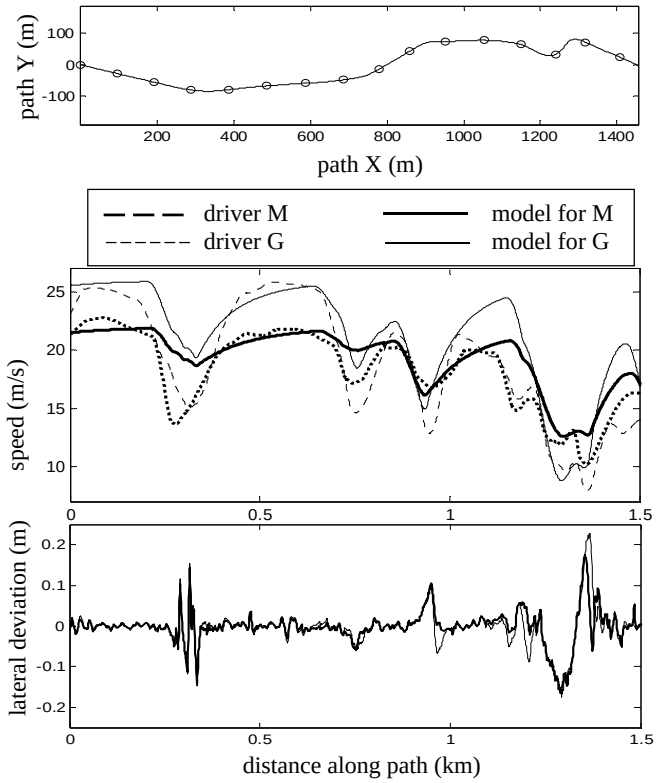

Fig. 6 : Driver model vs vehicle test data (predictive)

6. CONCLUDING REMARKS

The lateral controller is extremely effective given the stated objective of a simple yet realistic device. The algorithm is intuitively close to real driving behaviour and is simple to execute. The lateral robustness study yields results which verify that the single point lookahead is consistent with real driving, showing low sensitivity to the control gain, and successful, realistic path tracking into the nonlinear handling region. The lateral response is also robust to a simple track description process, and the algorithm operates in a computationally efficient way, considering only relevant sections of the track at each control timestep.

The longitudinal controller is functionally successful, and can be tuned to approximate the actual speed traces of test drivers; large scale variations in driving style can be represented. The results also provide an effective illustration of the extent to which driving speed depends on the simple, single criterion of lookahead distance. This part of the algorithm is also posed in a computationally efficient way.

The lateral control is elegant, depending on just two or three parameters according to the speed and hence lateral acceleration profile of the driving. The mapping of lookahead distance to modeled forward speed is rather less elegant, and there remains scope for development of a more parametrically efficient process here. As it stands, the model can be easily and effectively tuned, but if condensed further it could be employed within a filter to identify driving style in real-time; such a filter would be of use in many applications, ranging for example from advanced driver assistance and chassis control systems to actuarial assessment of car insurance risk.

REFERENCES

[1] MacAdam, C.C., 1981, *'Application of an Optimal Preview Control for Simulation of Closed-loop Automobile Driving'* IEEE Transactions on Systems, Man, and Cybernetics, v11, 393-399.

[2] Sharp, R.S., Casanova D. and Symonds, P., 2000, *'A Mathematical Model for Driver Steering Control, with Design, Tuning and Performance Results'* Vehicle System Dynamics, v33, 289-326.

[3] Ungoren, A.Y., and Peng, H., 2005, *'An Adaptive Lateral Preview Driver Model'*, Vehicle System Dynamics, v43, 245-259.

[4] Lee, T., Kang, J., Yi, K. and Noh, K., 2010, *'An Investigation on the Integrated Human Driver Model for Closed-loop Simulation of Intelligent Safety Systems'*, Journal of Mechanical Science and Technology, v24 761-767.

[5] Gordon, T.J., and Best, M.C., 2007, *'On the Synthesis of Driver Inputs for the Simulation of Closed-loop Handling Manoeuvres'*, International Journal of Vehicle Design, v40, 52-76.

[6] Nakashima, T., Tsubokura, M., Ikenaga, T. and Doi, Y., 2010, *'HPC-LES for Unsteady Aerodynamics of a Heavy Duty Truck in Wind Gust'*, SAE Technical Paper Series, 2010-01-1021

[7] Dixon, J.C., 1996, *'Tires, Suspension and Handling (Ed 2, Appendix C)'*, SAE Press.